



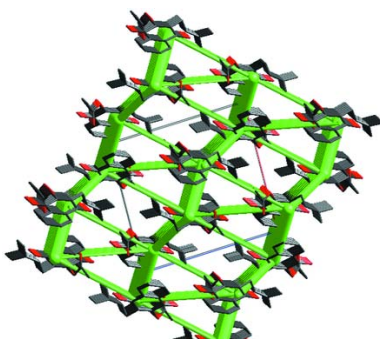
Received 5 August 2019
Accepted 13 August 2019

Edited by J. Ellena, Universidade de São Paulo,
Brazil

Keywords: crystal structure; naphthoquinone;
lapachol acetate; synthesis; Hirshfeld analysis.

CCDC reference: 1947085

Supporting information: this article has
supporting information at journals.iucr.org/e



OPEN ACCESS

Crystal structure and Hirshfeld surface analysis of lapachol acetate 80 years after its first synthesis

Miguel A. Martínez-Cabrera,^a Mario A. Macías,^b Francisco Ferreira,^c Enrique Pandolfi,^d Javier Barúa^e and Leopoldo Suescun^{f*}

^aUniversidad Nacional de Asunción, Facultad de Ciencias Exactas y Naturales, Departamento de Biología, Área Química Orgánica de los Productos Naturales-LAREV, San Lorenzo Campus-UNA, Paraguay, ^bDepartment of Chemistry, Universidad de los Andes, Cra 1 N° 18A-12, 111711, Bogotá, Colombia, ^cUniversidad Nacional de Asunción, Facultad de Ciencias Exactas y Naturales, Laboratorio de Análisis Instrumental, Departamento de Química, San Lorenzo Campus-UNA, Paraguay, ^dLaboratorio de Síntesis Orgánica, DQO, Facultad de Química, Universidad de la República, Montevideo 11800, Uruguay, ^eUniversidad Nacional de Asunción, Facultad de Ciencias Químicas, San Lorenzo Campus-UNA, Paraguay, and ^fCryssmat-Lab/DETEMA, Facultad de Química, Universidad de la República, Av. Gral. Flores 2124, Montevideo 11800, Uruguay. *Correspondence e-mail: leopoldo@fq.edu.uy

Lapachol acetate [systematic name: 3-(3-methylbut-2-enyl)-1,4-dioxonaphthalen-2-yl acetate], $C_{17}H_{16}O_4$, was prepared using a modified high-yield procedure and its crystal structure is reported for the first time 80 years after its first synthesis. The full spectroscopic characterization of the molecule is reported. The molecular conformation shows little difference with other lapachol derivatives and lapachol itself. The packing is directed by intermolecular $\pi-\pi$ and C–H···O interactions, as described by Hirshfeld surface analysis. The former interactions make the largest contributions to the total packing energy in a ratio of 2:1 with respect to the latter.

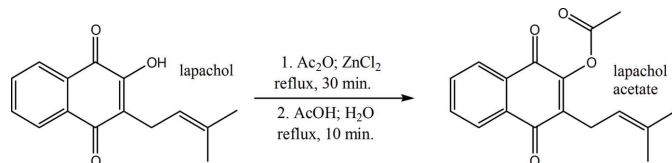
1. Chemical context

Naphthoquinones are natural products characterized by a naphthalene ring system exhibiting a *para*-quinone motif in positions 1,4. They are natural pigments and normally substituted by hydroxyl or methyl groups or present as glycosides (Bruneton, 2001). Among the natural products, they possess remarkable biological activity such as antibacterial, antifungal, antiparasitic, antiviral and anticancer (Babula *et al.*, 2007; da Silva & Ferreira, 2016; Miranda *et al.*, 2019; Araújo *et al.*, 2019; Barbosa Coitinho *et al.*, 2019; Strauch *et al.*, 2019). Lapachol (2-hydroxy-3-(3-methyl-but-2-enyl)-[1,4]naphthoquinone), isolated from *Handroanthus Heptaphyllus* (Vell.) Mattos, a native species from Paraguay, was studied as a hemisynthetic precursor of lapachol acetate {[3-(3-methyl-but-2-enyl)-1,4-dioxonaphthalen-2-yl]acetate} for the first time by Cooke *et al.* (1939). Jacobsen & Torsell (1973) prepared lapachol acetate using 2-acetoxy-1,4-naphthoquinone as a precursor with 79% yield. We developed an optimization of the first synthesis of lapachol acetate developed by Cooke *et al.* (1939), introducing several modifications with the purpose of standardizing it and increasing the yield to 97.5%. Details of the synthesis and the spectroscopic characterization are included in the supporting information. Noting that the crystal structure of lapachol acetate had not been reported, we also undertook the crystallization and structure determination.

2. Structural commentary

The lapachol acetate molecule (Fig. 1) is the ester of lapachol at the alcohol moiety (O2 in Larsen *et al.*, 1992). The molecule

is composed of three planar groups, the naphthoquinone nucleus comprising atoms C1 to C11, O1, O2 and O4, and two smaller butenyl and acetate residues at the sides. The butenyl and acetate mean planes are inclined to the naphthoquinone mean plane by 65.80 (10) and 78.52 (11) $^{\circ}$, respectively. The lapachol acetate molecule shows typical bond distances and angles, and overlaps very closely with the common part of the lapachol molecule in the structure LAPA II reported by Larsen *et al.* (1992) (Fig. 2), with an average deviation of C/O atomic positions of 0.158 \AA and a maximum deviation of 0.309 \AA for atom O4. This is rather unexpected, since the butenyl moiety shows rotational flexibility around the C3–C11 and C11–C12 bonds. However, in both reported lapachol polymorphs (Larsen *et al.*, 1992) and two derivatives (Eyong *et al.*, 2015; da Silva *et al.*, 2012) reported in the CSD (Groom *et al.*, 2016) with the same rotational freedom, the dihedral angle between the planar $\text{C}=\text{C}(\text{CH}_3)_2$ group and the naphthoquinone nucleus is close to 70 $^{\circ}$, as observed in lapachol acetate.



3. Supramolecular features

Crystals of lapachol acetate are held together by weak dipolar and dispersion forces because there is no strong H-donor residue in the molecule. Molecules connect with other units through weak $\text{C}(sp^3)\text{—H}\cdots\text{O}=\text{C}$ hydrogen bonds H11B···O4ⁱ and H15A···O1ⁱⁱ (Table 1, Fig. S4a in the supporting information) defining double sheets of molecules parallel to $(\bar{1}01)$. The butenyl residue of a screw-rotation-

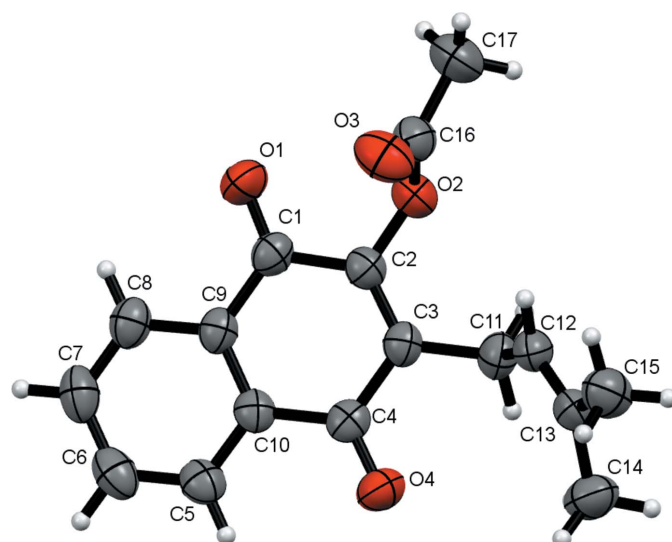


Figure 1

ORTEP view of a lapachol acetate molecule with the labelling scheme, and displacement ellipsoids drawn at the 50% probability level. One of the two positions of the disordered C17 methyl group has been omitted for clarity.

Table 1
Hydrogen-bond geometry (\AA , $^{\circ}$).

$D\text{—H}\cdots A$	$D\text{—H}$	$H\cdots A$	$D\cdots A$	$D\text{—H}\cdots A$
C11—H11B···O4 ⁱ	0.97	2.55	3.274 (3)	131
C15—H15A···O1 ⁱⁱ	0.96	2.59	3.485 (3)	156

Symmetry codes: (i) $-x + \frac{1}{2}, y - \frac{1}{2}, -z + \frac{3}{2}$; (ii) $x + \frac{1}{2}, -y + \frac{1}{2}, z + \frac{1}{2}$.

related molecule adds an intermolecular $\pi\text{—}\pi$ interaction with the naphthoquinone residue to the sheets with atoms C12ⁱⁱⁱ and C13ⁱⁱⁱ located at 3.243 and 3.544 \AA , respectively, from the naphthoquinone plane (Fig. S4b). Finally, the double sheets stack along the $[101]$ direction where naphthoquinone nuclei of inversion-related molecules display $\pi\text{—}\pi$ interactions. Ring 1 (C1–C4/C10/C9; centroid $Cg1$) of the molecule is close to ring 2 (C5–C10; centroid $Cg2$), the $Cg2\cdots Cg1^{iv}$ distance being 3.8532 (12) \AA ; $Cg2\cdots Cg2^{iv}$ is the shortest distance [3.8035 (13) \AA], with an average perpendicular distance between naphthoquinone planes of 3.3787 (9) \AA , as shown in Fig. S4c [symmetry codes: (i) $-x + \frac{1}{2}, y - \frac{1}{2}, -z + \frac{3}{2}$; (ii) $x + \frac{1}{2}, -y + \frac{1}{2}, z + \frac{1}{2}$; (iii) $\frac{1}{2} - x, \frac{1}{2} + y, \frac{3}{2} - z$; (iv) $1 - x, 1 - y, 1 - z$]. Considering the Hirshfeld (HF) surface (Turner *et al.*, 2017) mapped over d_{norm} (analysis of the contact distances d_i and d_e from the HF surface to the nearest atom inside and outside, respectively), these interactions in one molecule are shown in Fig. 3a and the sheets of molecules defined by them in Fig. 3b. The 2D fingerprints of lapachol acetate (shown in Fig. S5 of the supporting information) show no particular features other than the aforementioned $\text{H}\cdots\text{O}/\text{O}\cdots\text{H}$ contacts, which comprise 28.2% of the total HF surface, revealing their importance in the formation of the crystal.

In order to describe these interactions in a whole-of-molecule approach, accurate model energies of the interactions between molecules of lapachol acetate in the crystal were analysed. The interactions were calculated using the B3LYP/6–31 G(d,p) energy model implemented in *CrystalExplorer* (Turner *et al.*, 2017), which uses quantum mechanical charge distributions for unperturbed molecules (Mackenzie *et al.*, 2017). In the calculations, the total energy is modelled as the

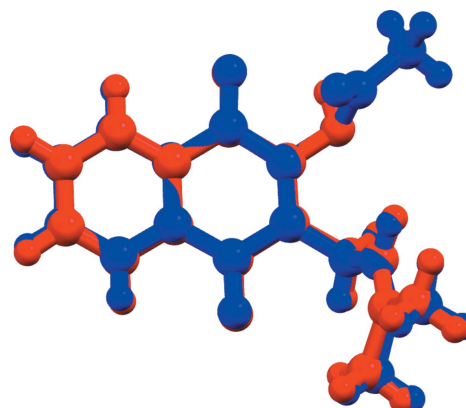
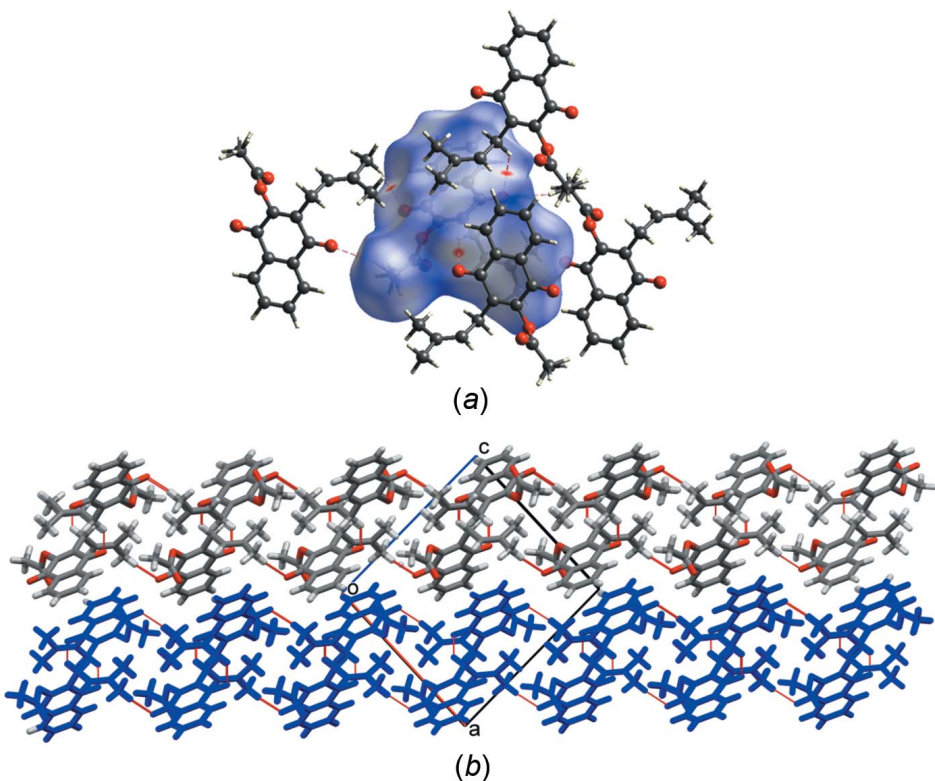
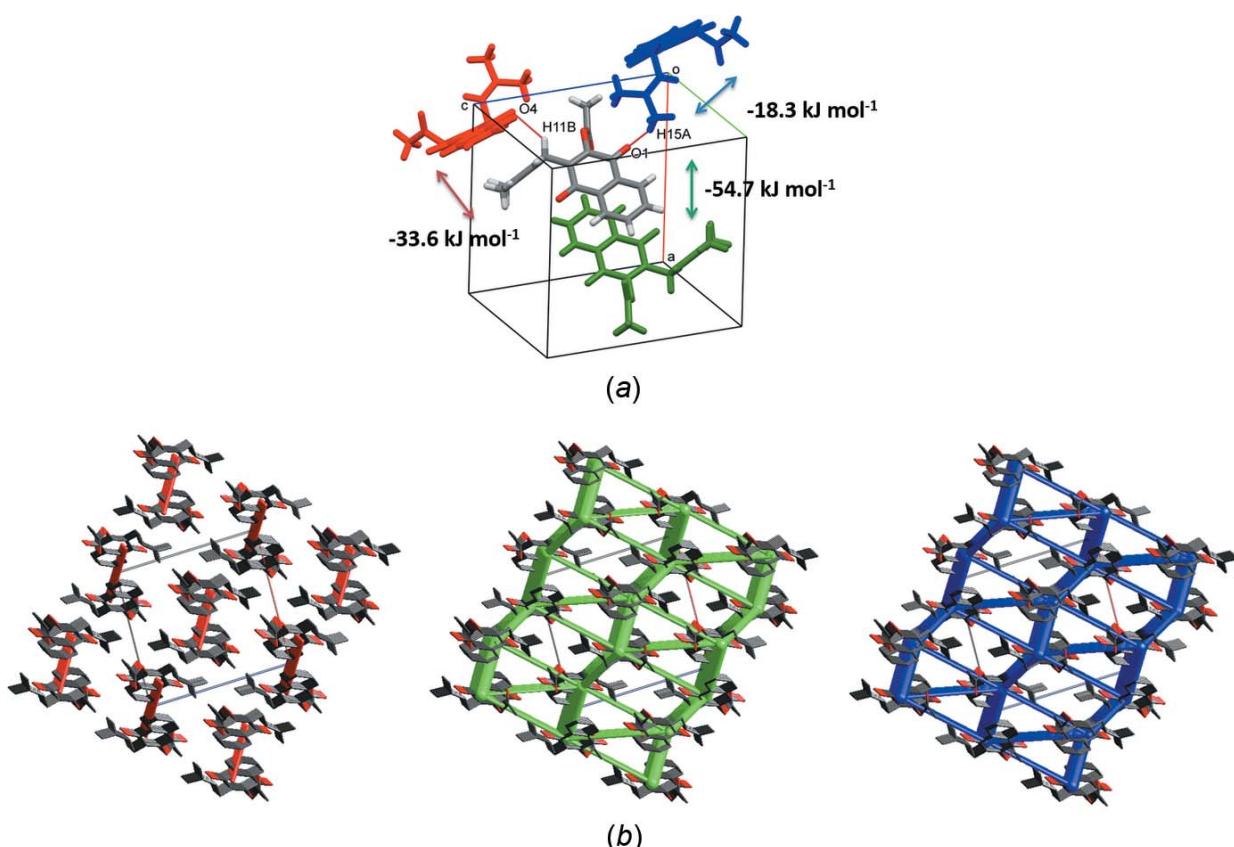


Figure 2

Overlay of a lapachol acetate (blue) and a lapachol (red) molecule (LAPA II molecule as described by Larsen *et al.*, 1992). Only the common C/O atoms were fitted.

**Figure 3**

(a) View of the Hirshfeld surface for lapachol acetate mapped over d_{norm} showing the C—H \cdots O hydrogen-bond interactions. (b) The molecular structure of lapachol acetate showing the formation of stacked (011) sheets.

**Figure 4**

(a) Molecular close contacts and (b) energy-framework diagrams for electrostatic (red) and dispersion (green) contributions to the total interaction energy (blue) in lapachol acetate crystals.

sum of the electrostatic (E_{ele}), polarization (E_{pol}), dispersion (E_{dis}) and exchange-repulsion (E_{rep}) terms (Mackenzie *et al.*, 2017). The strongest pairwise interaction with a total energy of $-54.7 \text{ kJ mol}^{-1}$ corresponds to the interaction between neighbouring aromatic systems, while the molecules connected through a combination of $\pi-\pi$ interactions between the butenyl and naphtoquinone residues and C11—H11B \cdots O4ⁱ hydrogen bonds have a total energy of $-33.6 \text{ kJ mol}^{-1}$. The weakest interaction, C15—H15A \cdots O1ⁱⁱ, shows a total energy of $-18.3 \text{ kJ mol}^{-1}$ (Fig. 4a). The energy framework diagrams for lapachol acetate (Fig. 4b) show that electrostatic forces act to keep pairs of inversion-related chains of molecules joined while dispersion forces act in three dimensions to build the crystal structure. The total energy diagram shows a high resemblance to the dispersion framework, showing that these forces are the most important in the crystal. The interaction energies for selected molecular pairs in the first coordination sphere around the asymmetric unit are summarized in Table S1 and Fig. S6 of the supporting information.

4. Database survey

Lapachol and its derivatives are rather scarce in the Cambridge Crystal Structure Database (Version 5.40, update 2 of May 2019; Groom *et al.*, 2016) with only 31 entries matching the basic C—O framework of lapachol. Two lapachol polymorphs LAPA I and LAPA II (Larsen *et al.*, 1992) have been reported at 105 K, as mentioned above. Two additional lapachol derivatives obtained by replacing one H atom have been reported during the current decade: 4-(3-hydroxy-1,4-dioxo-1,4-dihydronephthalen-2-yl)-2-methylbut-2-enal (Eyong *et al.*, 2015) is an aldehyde of lapachol at C15 and 3-(3-methylbut-2-en-1-yl)-1,4-dioxo-1,4-dihydronephthalen-2-yl 4-methylbenzenesulfonate (Silva *et al.*, 2012) is a sulfonate at O2. Lapachol acetate is the third derivative of this kind reported. Some lapachol derivatives where cyclization of the 3-methy-2-butenyl moiety or coordination with metals (as lapacholate) have additionally been reported, but are not related to lapachol acetate.

5. Synthesis and crystallization

Lapachol was obtained from an extract of *Handroanthus Heptaphyllus* (Vell.) Mattos, the pink trumpet tree (or lapacho negro) as described in the supporting information. 201 mg (0.823 mmol) of lapachol were dissolved in 5 ml of dry acetic anhydride and a catalytic amount of dry zinc chloride (ZnCl_2) was added. The suspension was refluxed for 30 min under an inert atmosphere (N_2). The solution was allowed to cool and 5 ml of glacial acetic acid and later 50 ml of distilled water were added. The final mixture was refluxed for 10 min and allowed to precipitate overnight. The crude solid was filtered, dried and purified by column chromatography (hexane: AcOEt, 9: 1 v/v) to obtain pure lapachol acetate as yellow crystals (see the detailed description of the obtention of lapachol and the synthesis of lapachol acetate in the

Table 2
Experimental details.

Crystal data	
Chemical formula	$\text{C}_{17}\text{H}_{16}\text{O}_4$
M_r	284.30
Crystal system, space group	Monoclinic, $P2_1/n$
Temperature (K)	296
a, b, c (Å)	12.0914 (8), 9.4741 (6), 12.7761 (9)
β (°)	92.943 (4)
V (Å ³)	1461.64 (17)
Z	4
Radiation type	Cu $K\alpha$
μ (mm ⁻¹)	0.75
Crystal size (mm)	0.26 × 0.22 × 0.18
Data collection	
Diffractometer	Bruker D8 Venture/Photon 100 CMOS
Absorption correction	Multi-scan (<i>SADABS</i> ; Krause <i>et al.</i> , 2015)
T_{\min}, T_{\max}	0.654, 0.754
No. of measured, independent and observed [$I > 2\sigma(I)$] reflections	7496, 2996, 1972
R_{int}	0.038
(sin θ/λ) _{max} (Å ⁻¹)	0.637
Refinement	
$R[F^2 > 2\sigma(F^2)], wR(F^2), S$	0.048, 0.136, 1.03
No. of reflections	2996
No. of parameters	193
H-atom treatment	H-atom parameters constrained
$\Delta\rho_{\text{max}}, \Delta\rho_{\text{min}}$ (e Å ⁻³)	0.17, -0.16

Computer programs: *APEX2* and *SAINT* (Bruker, 2014), *SHELXT* (Sheldrick, 2015a), *SHELXL2018* (Sheldrick, 2015b), *Mercury* (Macrae *et al.*, 2008) and *publCIF* (Westrip, 2010).

supporting information and the detailed spectroscopic study in Figs. S1–S3). Adequate crystals for diffraction were obtained by dissolving a few mg of the solid in a minimum amount of AcOEt in a rubber-stop vial with a syringe needle through the center to promote slow evaporation of the solvent at room temperature.

6. Refinement

Crystal data, data collection and structure refinement details are summarized in Table 2. H atoms were placed in calculated positions (C—H = 0.93–0.97 Å) and included as riding contributions, with isotropic displacement parameters set at 1.2–1.5 times the U_{eq} value of the parent atom. The C17 methyl group shows rotational disorder that was modelled with two positions that were refined with a fixed C—H bond distance but with rotational freedom (AFIX 147) converging at occupancies of 0.79 (3) and 0.21 (3).

Acknowledgements

The authors are indebted to N. Di Benedetto for her contribution to the single-crystal X-ray diffraction data processing and to G. Cebrán-Torrejón for his assistance in the spectroscopic characterization. Funding for this research was provided by Programa de Desarrollo de Ciencias Basicas - PEDECIBA - Uruguay (grant to Leopoldo Suescum, Enrique

Pandolfi); Facultad de Ciencias Exactas y Naturales, Universidad Nacional de Asunción (Paraguay).

References

- Araújo, I. A. C., de Paula, R. C., Alves, C. L., Faria, K. F., Oliveira, M. M., Mendes, G. G., Dias, E. M. F. A., Ribeiro, R. R., Oliveira, A. B. & Silva, S. M. D. (2019). *Exp. Parasitol.* **199**, 67–73.
- Babula, P., Adam, V., Havel, L. & Kizek, R. (2007). *Ceska Slov Farm Cas Ceske Farm Spolecnosti Slov Farm Spolecnosti*, **56**, 114–20.
- Barbosa Coitinho, L., Fumagalli, F., da Rosa-Garzon, N. G., da Silva Emery, F. & Cabral, H. (2019). *Prep. Biochem. Biotechnol.* **49**, 459–463.
- Bruker (2014). *APEX2, SAINT and SADABS*. Bruker AXS Inc., Madison, Wisconsin, USA.
- Bruneton, J. (2001). *Farmacognosia. Fitoquímica. Plantas medicinales*, edited by A. Villar del Fresno, E. Carretero and M. Rebuelta. Spain: ACRIBIA Editorial S. A.
- Cooke, R. G., Macbeth, A. K. & Winzor, F. L. (1939). *J. Chem. Soc.* pp. 878–884.
- Eyong, K. O., Ketsemen, H. L., Ghansenuy, S. Y. & Folefoc, G. N. (2015). *Med. Chem. Res.* **24**, 965–969.
- Groom, C. R., Bruno, I. J., Lightfoot, M. P. & Ward, S. C. (2016). *Acta Cryst. B* **72**, 171–179.
- Jacobsen, N. & Torsell, K. (1973). *Acta Chem. Scand.* **27**, 3211–3216.
- Krause, L., Herbst-Irmer, R., Sheldrick, G. M. & Stalke, D. (2015). *J. Appl. Cryst.* **48**, 3–10.
- Larsen, I. K., Andersen, L. A. & Pedersen, B. F. (1992). *Acta Cryst. C* **48**, 2009–2013.
- Mackenzie, C. F., Spackman, P. R., Jayatilaka, D. & Spackman, M. A. (2017). *IUCrJ*, **4**, 575–587.
- Macrae, C. F., Bruno, I. J., Chisholm, J. A., Edgington, P. R., McCabe, P., Pidcock, E., Rodriguez-Monge, L., Taylor, R., van de Streek, J. & Wood, P. A. (2008). *J. Appl. Cryst.* **41**, 466–470.
- Miranda, S. E., Lemos, J. A., Fernandes, R. S., Ottoni, F. M., Alves, R. J., Ferretti, A., Rubello, D., Cardoso, V. N. & Branco de Barrosa, A. L. (2019). *Rev. Esp. Med. Nucl. Ima.* **38**, 167–172.
- Sheldrick, G. M. (2015a). *Acta Cryst. A* **71**, 3–8.
- Sheldrick, G. M. (2015b). *Acta Cryst. C* **71**, 3–8.
- Silva, E. N. da de Júnior, Melo, I. M. M., Diogo, E. B. T., Costa, V. A., de Souza Filho, J. D., Valença, W. O., Camara, C. A., de Oliveira, R. N., de Araujo, A. S., Emery, F. S., dos Santos, M. R., de Simone, C. A., Menna-Barreto, R. F. S. & de Castro, S. L. (2012). *Eur. J. Med. Chem.* **52**, 304–312.
- Silva, F. C. da & Ferreira, V. F. (2016). *Curr. Org. Synth.* **13**, 334–371.
- Strauch, M. A., Tomaz, M. A., Monteiro-Machado, M., Cons, B. L., Patrão-Neto, F. C., Teixeira-Cruz, J. D. M., Tavares-Henriques, M. D. S., Nogueira-Souza, P. D., Gomes, S. L. S., Costa, P. R. R., Schaeffer, E., da Silva, A. J. M. & Melo, P. A. (2019). *PLoS One*, **14**, e0211229.
- Turner, M. J., McKinnon, J. J., Wolff, S. K., Grimwood, D. J., Spackman, P. R., Jayatilaka, D. & Spackman, M. A. (2017). *CrystalExplorer17*. University of Western Australia. <http://hirshfeldsurface.net>.
- Westrip, S. P. (2010). *J. Appl. Cryst.* **43**, 920–925.

supporting information

Acta Cryst. (2019). E75, 1362-1366 [https://doi.org/10.1107/S2056989019011393]

Crystal structure and Hirshfeld surface analysis of lapachol acetate 80 years after its first synthesis

Miguel A. Martínez-Cabrera, Mario A. Macías, Francisco Ferreira, Enrique Pandolfi, Javier Barúa and Leopoldo Suescun

Computing details

Data collection: *APEX2* (Bruker, 2014); cell refinement: *SAINT* (Bruker, 2014); data reduction: *SAINT* (Bruker, 2014); program(s) used to solve structure: *SHELXT* (Sheldrick, 2015a); program(s) used to refine structure: *SHELXL2018* (Sheldrick, 2015b); molecular graphics: *Mercury* (Macrae *et al.*, 2008); software used to prepare material for publication: *publCIF* (Westrip, 2010).

3-(3-Methylbut-2-enyl)-1,4-dioxonaphthalen-2-yl acetate

Crystal data

$C_{17}H_{16}O_4$
 $M_r = 284.30$
Monoclinic, $P2_1/n$
 $a = 12.0914 (8)$ Å
 $b = 9.4741 (6)$ Å
 $c = 12.7761 (9)$ Å
 $\beta = 92.943 (4)$ °
 $V = 1461.64 (17)$ Å³
 $Z = 4$
 $F(000) = 600$

$D_x = 1.292$ Mg m⁻³
Melting point: 352(1) K
Cu $K\alpha$ radiation, $\lambda = 1.54178$ Å
Cell parameters from 7958 reflections
 $\theta = 4.9\text{--}75.7$ °
 $\mu = 0.75$ mm⁻¹
 $T = 296$ K
Block, yellow
0.26 × 0.22 × 0.18 mm

Data collection

Bruker D8 Venture/Photon 100 CMOS diffractometer
Radiation source: Cu Incoatec microsource
Detector resolution: 10.4167 pixels mm⁻¹
 $\backslash j$ and ω scans
Absorption correction: multi-scan (SADABS; Krause *et al.*, 2015)
 $T_{\min} = 0.654$, $T_{\max} = 0.754$

7496 measured reflections
2996 independent reflections
1972 reflections with $I > 2\sigma(I)$
 $R_{\text{int}} = 0.038$
 $\theta_{\max} = 79.2$ °, $\theta_{\min} = 4.9$ °
 $h = -13 \rightarrow 15$
 $k = -11 \rightarrow 9$
 $l = -16 \rightarrow 15$

Refinement

Refinement on F^2
Least-squares matrix: full
 $R[F^2 > 2\sigma(F^2)] = 0.048$
 $wR(F^2) = 0.136$
 $S = 1.03$
2996 reflections
193 parameters
0 restraints

Primary atom site location: dual
Secondary atom site location: difference Fourier map
Hydrogen site location: inferred from neighbouring sites
H-atom parameters constrained
 $w = 1/[\sigma^2(F_o^2) + (0.053P)^2 + 0.3463P]$
where $P = (F_o^2 + 2F_c^2)/3$

$(\Delta/\sigma)_{\max} < 0.001$
 $\Delta\rho_{\max} = 0.17 \text{ e } \text{\AA}^{-3}$

$\Delta\rho_{\min} = -0.16 \text{ e } \text{\AA}^{-3}$

Special details

Geometry. All esds (except the esd in the dihedral angle between two l.s. planes) are estimated using the full covariance matrix. The cell esds are taken into account individually in the estimation of esds in distances, angles and torsion angles; correlations between esds in cell parameters are only used when they are defined by crystal symmetry. An approximate (isotropic) treatment of cell esds is used for estimating esds involving l.s. planes.

Fractional atomic coordinates and isotropic or equivalent isotropic displacement parameters (\AA^2)

	x	y	z	$U_{\text{iso}}^*/U_{\text{eq}}$	Occ. (<1)
O1	0.22182 (14)	0.34297 (18)	0.34233 (12)	0.0686 (5)	
C1	0.25877 (15)	0.3726 (2)	0.42998 (15)	0.0468 (5)	
O2	0.17186 (11)	0.16221 (16)	0.49500 (11)	0.0540 (4)	
C2	0.24117 (15)	0.2761 (2)	0.51890 (15)	0.0441 (5)	
O3	0.30987 (14)	0.05735 (18)	0.41410 (15)	0.0756 (5)	
C3	0.28099 (15)	0.2973 (2)	0.61720 (15)	0.0443 (5)	
O4	0.39859 (12)	0.43627 (17)	0.72673 (11)	0.0586 (4)	
C4	0.35332 (15)	0.4218 (2)	0.64003 (14)	0.0440 (5)	
C5	0.42753 (17)	0.6488 (2)	0.57604 (17)	0.0529 (5)	
H5	0.460252	0.663841	0.642578	0.063*	
C6	0.43917 (18)	0.7485 (3)	0.49821 (19)	0.0615 (6)	
H6	0.479948	0.830043	0.512619	0.074*	
C7	0.39054 (19)	0.7275 (3)	0.39920 (19)	0.0612 (6)	
H7	0.397581	0.795506	0.347504	0.073*	
C8	0.33163 (17)	0.6057 (3)	0.37709 (17)	0.0547 (5)	
H8	0.299507	0.591249	0.310242	0.066*	
C9	0.32006 (15)	0.5041 (2)	0.45465 (15)	0.0444 (5)	
C10	0.36737 (15)	0.5268 (2)	0.55524 (15)	0.0426 (4)	
C11	0.26046 (18)	0.1969 (2)	0.70541 (16)	0.0533 (5)	
H11A	0.260239	0.249275	0.770631	0.064*	
H11B	0.188017	0.154157	0.693426	0.064*	
C12	0.34630 (17)	0.0828 (2)	0.71541 (16)	0.0505 (5)	
H12	0.350981	0.023269	0.657923	0.061*	
C13	0.41622 (17)	0.0566 (2)	0.79619 (16)	0.0510 (5)	
C14	0.4219 (2)	0.1431 (3)	0.89505 (18)	0.0719 (7)	
H14A	0.412225	0.082669	0.954178	0.108*	
H14B	0.364369	0.213071	0.891358	0.108*	
H14C	0.492685	0.188880	0.902682	0.108*	
C15	0.4952 (2)	-0.0652 (3)	0.7946 (2)	0.0684 (7)	
H15A	0.569682	-0.031304	0.805937	0.103*	
H15B	0.487694	-0.111606	0.727755	0.103*	
H15C	0.478890	-0.130827	0.848916	0.103*	
C16	0.2148 (2)	0.0591 (2)	0.43364 (17)	0.0557 (5)	
C17	0.1276 (2)	-0.0443 (3)	0.3994 (2)	0.0785 (8)	0.79 (3)
H17A	0.072901	0.001798	0.354279	0.118*	0.79 (3)
H17B	0.093164	-0.081079	0.459726	0.118*	0.79 (3)

H17C	0.160520	-0.120203	0.362194	0.118*	0.79 (3)
C17'	0.1276 (2)	-0.0443 (3)	0.3994 (2)	0.0785 (8)	0.21 (3)
H17D	0.058095	-0.016088	0.425921	0.118*	0.21 (3)
H17E	0.147328	-0.136138	0.426025	0.118*	0.21 (3)
H17F	0.121161	-0.047259	0.324252	0.118*	0.21 (3)

Atomic displacement parameters (\AA^2)

	U^{11}	U^{22}	U^{33}	U^{12}	U^{13}	U^{23}
O1	0.0903 (12)	0.0652 (12)	0.0484 (8)	-0.0047 (9)	-0.0162 (8)	0.0054 (8)
C1	0.0471 (10)	0.0480 (12)	0.0449 (11)	0.0085 (9)	-0.0009 (8)	0.0029 (9)
O2	0.0536 (8)	0.0488 (9)	0.0596 (8)	-0.0054 (7)	0.0025 (7)	-0.0014 (7)
C2	0.0430 (9)	0.0407 (11)	0.0486 (10)	0.0036 (9)	0.0025 (8)	0.0002 (9)
O3	0.0664 (10)	0.0607 (12)	0.1004 (13)	0.0026 (9)	0.0100 (9)	-0.0191 (10)
C3	0.0449 (10)	0.0430 (12)	0.0456 (10)	0.0058 (9)	0.0060 (8)	0.0037 (9)
O4	0.0653 (9)	0.0646 (11)	0.0452 (8)	0.0030 (8)	-0.0055 (7)	-0.0027 (7)
C4	0.0431 (10)	0.0448 (12)	0.0443 (10)	0.0105 (9)	0.0051 (8)	-0.0028 (9)
C5	0.0557 (12)	0.0456 (13)	0.0581 (12)	0.0034 (10)	0.0095 (10)	-0.0063 (11)
C6	0.0621 (13)	0.0424 (14)	0.0813 (16)	-0.0016 (11)	0.0171 (12)	-0.0029 (12)
C7	0.0673 (14)	0.0464 (14)	0.0715 (15)	0.0066 (11)	0.0198 (12)	0.0138 (12)
C8	0.0571 (12)	0.0534 (14)	0.0539 (12)	0.0109 (11)	0.0061 (9)	0.0098 (11)
C9	0.0457 (10)	0.0428 (12)	0.0452 (10)	0.0088 (9)	0.0065 (8)	0.0049 (9)
C10	0.0431 (9)	0.0373 (11)	0.0479 (10)	0.0086 (8)	0.0078 (8)	-0.0009 (9)
C11	0.0566 (12)	0.0559 (14)	0.0479 (11)	-0.0022 (10)	0.0067 (9)	0.0092 (10)
C12	0.0625 (12)	0.0431 (13)	0.0458 (10)	-0.0042 (10)	0.0010 (9)	0.0028 (9)
C13	0.0543 (11)	0.0490 (13)	0.0494 (11)	-0.0102 (10)	-0.0005 (9)	0.0040 (10)
C14	0.0739 (15)	0.086 (2)	0.0545 (13)	-0.0051 (14)	-0.0078 (11)	-0.0076 (13)
C15	0.0697 (14)	0.0583 (16)	0.0756 (15)	0.0019 (13)	-0.0109 (12)	0.0043 (13)
C16	0.0658 (13)	0.0453 (13)	0.0556 (12)	-0.0005 (11)	-0.0019 (10)	0.0025 (10)
C17	0.0874 (18)	0.0623 (18)	0.0851 (18)	-0.0195 (14)	-0.0028 (14)	-0.0071 (15)
C17'	0.0874 (18)	0.0623 (18)	0.0851 (18)	-0.0195 (14)	-0.0028 (14)	-0.0071 (15)

Geometric parameters (\AA , $^\circ$)

O1—C1	1.217 (2)	C11—C12	1.500 (3)
C1—C9	1.476 (3)	C11—H11A	0.9700
C1—C2	1.482 (3)	C11—H11B	0.9700
O2—C16	1.371 (3)	C12—C13	1.324 (3)
O2—C2	1.391 (2)	C12—H12	0.9300
C2—C3	1.337 (3)	C13—C15	1.499 (3)
O3—C16	1.189 (3)	C13—C14	1.504 (3)
C3—C4	1.489 (3)	C14—H14A	0.9600
C3—C11	1.505 (3)	C14—H14B	0.9600
O4—C4	1.218 (2)	C14—H14C	0.9600
C4—C10	1.487 (3)	C15—H15A	0.9600
C5—C6	1.384 (3)	C15—H15B	0.9600
C5—C10	1.384 (3)	C15—H15C	0.9600
C5—H5	0.9300	C16—C17'	1.488 (3)

C6—C7	1.382 (3)	C16—C17	1.488 (3)
C6—H6	0.9300	C17—H17A	0.9600
C7—C8	1.377 (3)	C17—H17B	0.9600
C7—H7	0.9300	C17—H17C	0.9600
C8—C9	1.394 (3)	C17'—H17D	0.9600
C8—H8	0.9300	C17'—H17E	0.9600
C9—C10	1.396 (3)	C17'—H17F	0.9600
O1—C1—C9	123.21 (19)	H11A—C11—H11B	107.9
O1—C1—C2	120.2 (2)	C13—C12—C11	127.8 (2)
C9—C1—C2	116.57 (16)	C13—C12—H12	116.1
C16—O2—C2	115.91 (16)	C11—C12—H12	116.1
C3—C2—O2	120.42 (18)	C12—C13—C15	121.0 (2)
C3—C2—C1	124.68 (19)	C12—C13—C14	123.5 (2)
O2—C2—C1	114.76 (16)	C15—C13—C14	115.45 (19)
C2—C3—C4	118.84 (18)	C13—C14—H14A	109.5
C2—C3—C11	122.93 (19)	C13—C14—H14B	109.5
C4—C3—C11	118.16 (17)	H14A—C14—H14B	109.5
O4—C4—C10	121.63 (19)	C13—C14—H14C	109.5
O4—C4—C3	119.97 (19)	H14A—C14—H14C	109.5
C10—C4—C3	118.40 (16)	H14B—C14—H14C	109.5
C6—C5—C10	120.2 (2)	C13—C15—H15A	109.5
C6—C5—H5	119.9	C13—C15—H15B	109.5
C10—C5—H5	119.9	H15A—C15—H15B	109.5
C7—C6—C5	120.4 (2)	C13—C15—H15C	109.5
C7—C6—H6	119.8	H15A—C15—H15C	109.5
C5—C6—H6	119.8	H15B—C15—H15C	109.5
C8—C7—C6	120.0 (2)	O3—C16—O2	121.9 (2)
C8—C7—H7	120.0	O3—C16—C17'	127.4 (2)
C6—C7—H7	120.0	O2—C16—C17'	110.7 (2)
C7—C8—C9	120.2 (2)	O3—C16—C17	127.4 (2)
C7—C8—H8	119.9	O2—C16—C17	110.7 (2)
C9—C8—H8	119.9	C16—C17—H17A	109.5
C8—C9—C10	119.8 (2)	C16—C17—H17B	109.5
C8—C9—C1	119.93 (18)	H17A—C17—H17B	109.5
C10—C9—C1	120.30 (18)	C16—C17—H17C	109.5
C5—C10—C9	119.48 (19)	H17A—C17—H17C	109.5
C5—C10—C4	119.83 (18)	H17B—C17—H17C	109.5
C9—C10—C4	120.69 (19)	C16—C17'—H17D	109.5
C12—C11—C3	112.29 (17)	C16—C17'—H17E	109.5
C12—C11—H11A	109.1	H17D—C17'—H17E	109.5
C3—C11—H11A	109.1	C16—C17'—H17F	109.5
C12—C11—H11B	109.1	H17D—C17'—H17F	109.5
C3—C11—H11B	109.1	H17E—C17'—H17F	109.5
C16—O2—C2—C3	-112.3 (2)	O1—C1—C9—C10	-175.23 (19)
C16—O2—C2—C1	71.8 (2)	C2—C1—C9—C10	6.1 (3)
O1—C1—C2—C3	178.0 (2)	C6—C5—C10—C9	1.0 (3)

C9—C1—C2—C3	−3.2 (3)	C6—C5—C10—C4	−178.70 (18)
O1—C1—C2—O2	−6.2 (3)	C8—C9—C10—C5	−1.5 (3)
C9—C1—C2—O2	172.54 (16)	C1—C9—C10—C5	177.96 (17)
O2—C2—C3—C4	−178.93 (16)	C8—C9—C10—C4	178.22 (17)
C1—C2—C3—C4	−3.4 (3)	C1—C9—C10—C4	−2.3 (3)
O2—C2—C3—C11	4.0 (3)	O4—C4—C10—C5	−4.1 (3)
C1—C2—C3—C11	179.59 (18)	C3—C4—C10—C5	175.37 (17)
C2—C3—C4—O4	−173.37 (18)	O4—C4—C10—C9	176.20 (18)
C11—C3—C4—O4	3.8 (3)	C3—C4—C10—C9	−4.4 (3)
C2—C3—C4—C10	7.2 (3)	C2—C3—C11—C12	88.5 (2)
C11—C3—C4—C10	−175.65 (17)	C4—C3—C11—C12	−88.5 (2)
C10—C5—C6—C7	0.3 (3)	C3—C11—C12—C13	118.3 (2)
C5—C6—C7—C8	−1.1 (3)	C11—C12—C13—C15	178.2 (2)
C6—C7—C8—C9	0.6 (3)	C11—C12—C13—C14	−1.0 (4)
C7—C8—C9—C10	0.7 (3)	C2—O2—C16—O3	9.9 (3)
C7—C8—C9—C1	−178.78 (19)	C2—O2—C16—C17'	−170.81 (18)
O1—C1—C9—C8	4.2 (3)	C2—O2—C16—C17	−170.81 (18)
C2—C1—C9—C8	−174.46 (17)		

Hydrogen-bond geometry (Å, °)

D—H···A	D—H	H···A	D···A	D—H···A
C11—H11B···O4 ⁱ	0.97	2.55	3.274 (3)	131
C15—H15A···O1 ⁱⁱ	0.96	2.59	3.485 (3)	156

Symmetry codes: (i) $-x+1/2, y-1/2, -z+3/2$; (ii) $x+1/2, -y+1/2, z+1/2$.